ICANS-XIII
13th Meeting of the International Collaboration on
Advanced Neutron Sources
October 11-14, 1995
Paul Scherrer Institut, 5232 Villigen PSI, Switzerland

THE NEW SMALL-ANGLE DIFFRACTOMETER SAND AT IPNS*

R. K. Crawford, P. Thiyagarajan, J. E. Epperson, F. Trouw, R. Kleb, D Wozniak, D. Leach
Argonne National Laboratory, Argonne, IL 60439 USA

ABSTRACT

A new small-angle neutron diffractometer SAND is undergoing commissioning at IPNS. This paper provides details of the design and expected performance of this instrument.

1. Introduction

In 1980, a prototype time-of-flight (TOF) small-angle diffractometer was operated at the prototype pulsed neutron source ZING-P' at Argonne National Laboratory, and this instrument was later upgraded and operated at the IPNS pulsed source from 1982 through 1984. In late 1984, this instrument was further upgraded to become the current Small Angle Diffractometer (SAD) at IPNS. Many experiments have been performed on the SAD by Argonne and outside users, and these have resulted in a number of publications to date. The quality of this work as well as that at other pulsed source small-angle neutron scattering (SANS) instruments clearly demonstrates that SANS using the TOF method at a pulsed source is now an established technique, capable of producing data of quality comparable to those taken on the more mature reactor instruments.

The SAD instrument at IPNS has been severely oversubscribed for several years, with proposals exceeding operating time by a factor of two to three. Because of this, and because experience led us to believe we could now build a significantly improved instrument, consideration of a second SANS instrument at IPNS was begun in 1986. Design of this second small-angle diffractometer and development of the necessary components has proceeded with relatively low priority, but the new instrument (named SAND) is now beginning commissioning. A number of related studies have also been completed during this period.[1-8]

* Work supported by U.S. Department of Energy, BES, contract No. W-31-109-ENG-38.

Keywords: Small-angle, Instrument, Collimation

The new instrument SAND is designed to provide all the capabilities now provided by SAD, and to enhance those capabilities by extending the dynamic range and improving the ease of operation and the instrument reliability. One goal is to make a value of Q_{min} down to 0.002 $Å^{-1}$ readily accessible for those experiments which require it. Since for small scattering angles ϕ

$$Q \approx \frac{2\pi\phi}{\lambda} \tag{1}$$

the minimum Q which can be reached is

$$Q_{min} \approx \frac{2\pi\phi_{min}}{\lambda_{max}} \tag{2}$$

Thus to reduce Q_{min} from that on SAD (~0.005 $Å^{-1}$), one must either use tighter collimation of the incident beam (to reduce ϕ_{min}) or longer wavelengths (to increase λ_{max}) or both. The new instrument includes a chopper to allow operation with much longer wavelengths, and will eventually have a second set of collimators having smaller angular divergence, both of which will serve to reduce Q_{min}.

A second goal is to increase the maximum Q value accessible, and to provide better counting statistics for the higher Q data where the scattering cross-section is usually quite small. For a given wavelength, Q_{max} can be increased only by increasing the maximum scattering angle which can be used. This goal has already been partially addressed by procuring a 40 cm × 40 cm detector for the new instrument. This is twice the linear dimensions of the SAD detector (4 times the area). An array of linear position-sensitive detectors (LPSDs) at higher scattering angles is also included to provide large additional increases in Q_{max}.

Experience with SAD has suggested a number of improvements which would enhance the instrument operation. Based on these suggestions, SAND includes features to facilitate the alignment of the instrument components and of the sample, improved access for various types of sample environment equipment, and design features to permit *in situ* calibration of the area detector.

This paper presents details of the SAND instrument, indicating differences from SAD where appropriate. Some examples of SAD data are presented, and expected improvements with SAND are discussed.

2. SAND Design

2.1 Overview

Figure 1 shows SAND in its location on the C3 beamline, and indicates its relationship to its neighbors. Figures 2 and 3 show portions of the instrument in greater detail, indicating the geometry and relative placement of major components of the instrument. Major components include the moderator, incident beam filter, background chopper, collimation system, sample chamber, area detector, high-angle detector bank, and beam monitors and beamstops. Specifications for various components and the reasoning behind their designs are discussed below. Table 1 summarizes the instrument parameters for SAND.

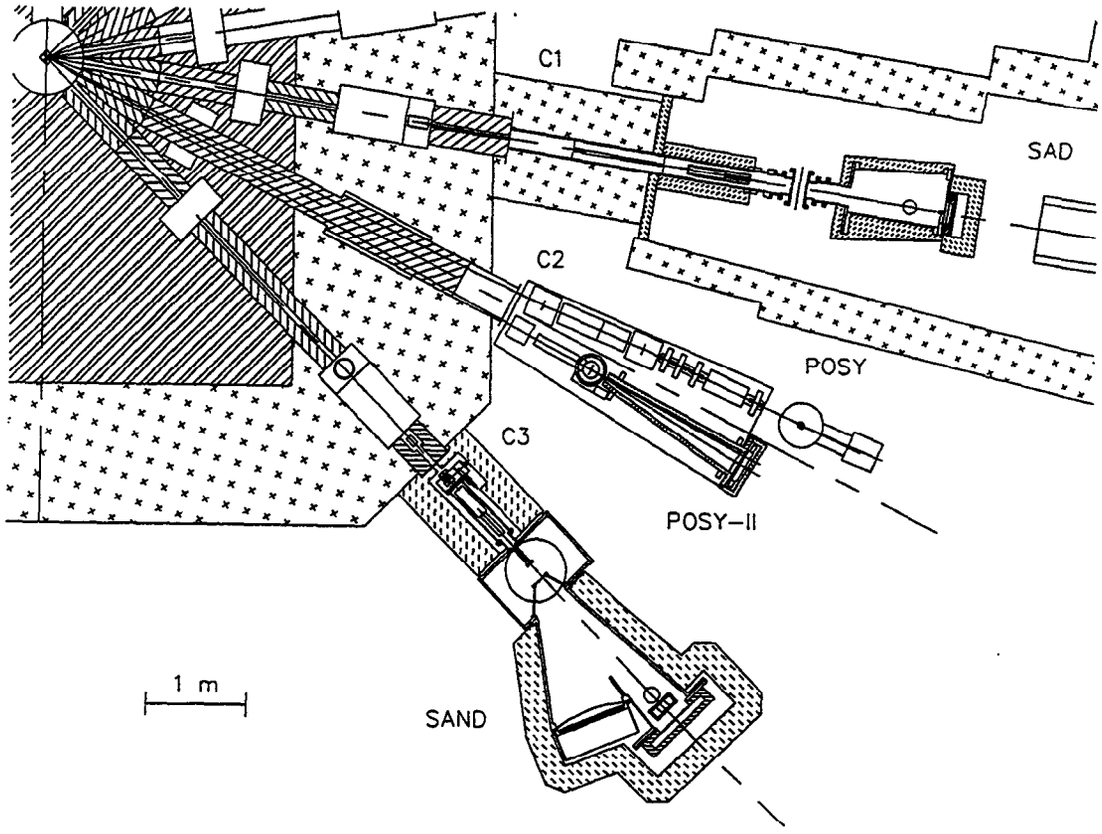

Figure 1. Top view of a portion of the IPNS experiment hall, showing SAND and adjacent instruments.

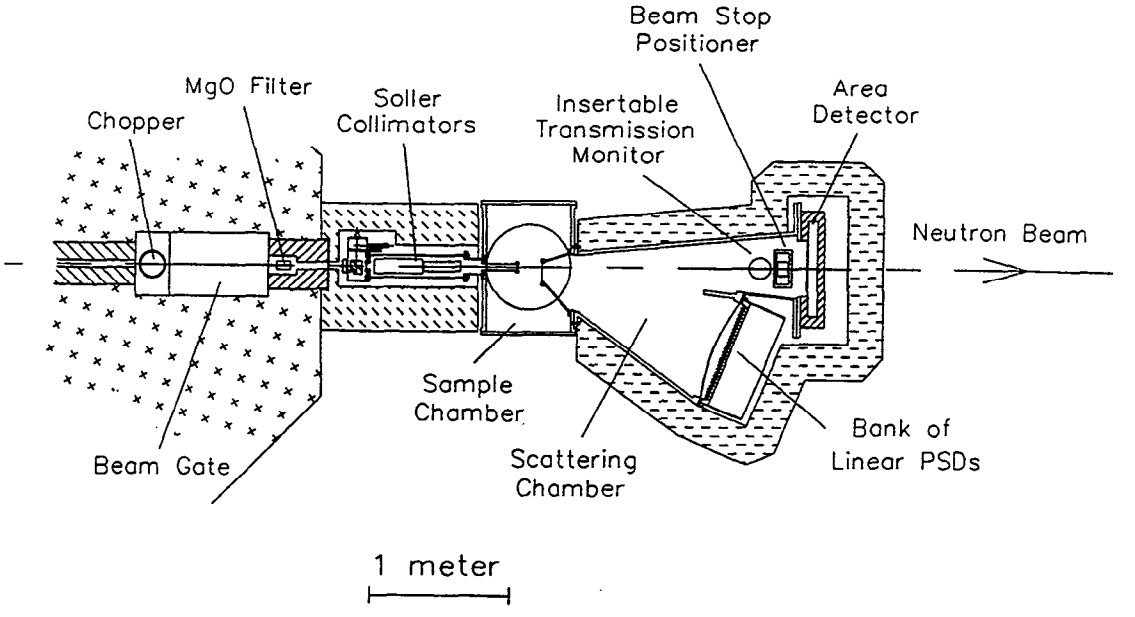

Figure 2. Top view of SAND, showing major instrument components.

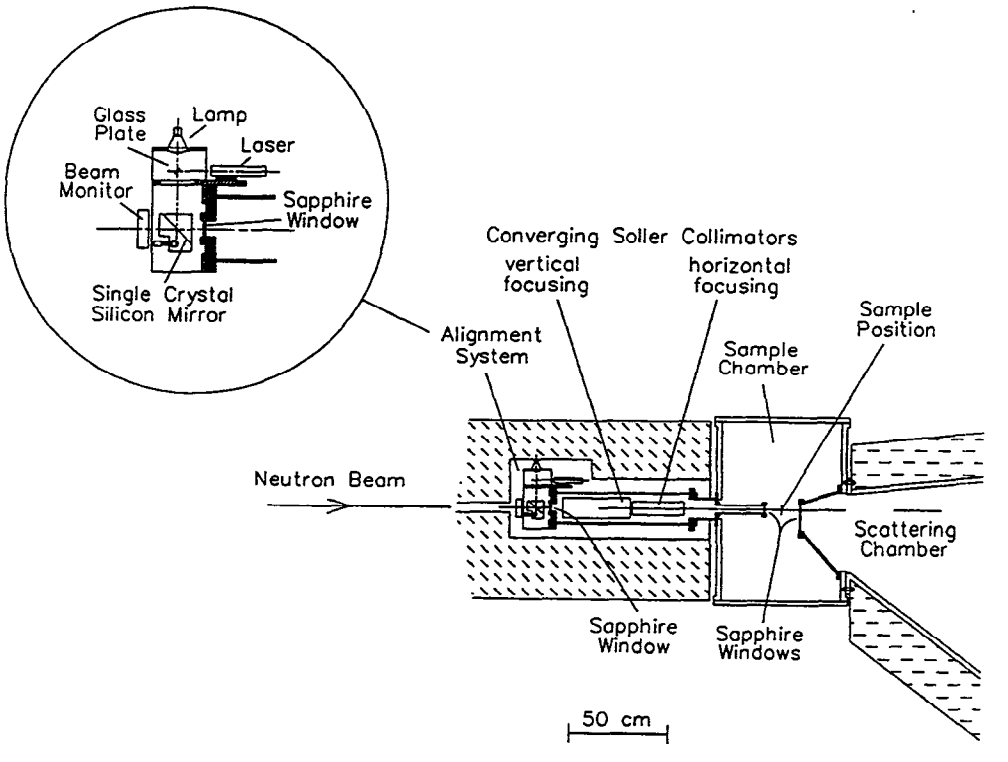

Figure 3. Details of the collimation and alignment systems on SAND. The inset shows a ×2 magnification of the optical alignment system and the incident beam monitor.

Table 1. Parameters for SAND

Parameter	Value
Source frequency	30 Hz
Moderator	decoupled solid CH_4
Source-to-sample distance	7.0 m
Sample-to-area-detector distance	2.0 m
Collimator-to-sample distance	0.5 m
Sample-to-LPSD distance	1.524 m
Beam size at moderator	9.0-cm diameter
Maximum beam size at sample	2.0-cm diameter
Area detector	
active area	40×40 cm^2
active thickness	2.5 cm
resolution	4-6 mm
fill	2.6 atm ^{3}He plus 1.4 atm CF_4
encoding	rise time, 256×256 pixels
max. scattering angle	~9°
LPSD	
active volume per detector	1.1 cm diameter × 60 cm long
number of detectors	65
resolution	1-2 cm along detector
fill	~10 atm ^{3}He
encoding	charge division, 64 segments/ detector
max. scattering angle	36°
Focusing collimators	
coarse	0.0034 radians fwhm
fine	0.0014 radians fwhm
Wavelength range	1-14 Å (5-14 Å for crystalline samples)
Q_{max}	
λ_{min} = 1.0 Å (noncrystalline)	>2.0 Å^{-1}
λ_{min} = 5.0 Å (crystalline)	~0.6 Å^{-1}
Q_{min} (λ_{max} = 14 Å)	
coarse collimation	~0.005 Å^{-1}
fine collimation	~0.002 Å^{-1}
Q_{min} (λ_{max} = 28 Å, using chopper)	
coarse collimation	~0.003 Å^{-1}
fine collimation	~0.001 Å^{-1}

2.2 Moderator

The C3 beamline where SAND is located is one of three beamlines viewing the same cold moderator. SAD on beamline C1 also views the same moderator, as do POSY and POSY-II. From early 1985 until late 1988, and again since 1994, these beamlines have viewed a grooved solid CH_4 moderator (physical temperature ~ 20 K) which is an excellent source of long-wavelength neutrons. During the other operating periods, the moderator can was filled with liquid H_2 instead. Measurements shown in Fig. 4 indicate that over most of the wavelength range of interest for small-angle diffraction the solid CH_4 moderator provides a factor of ~3.5 more intensity than did the liquid H_2 moderator.

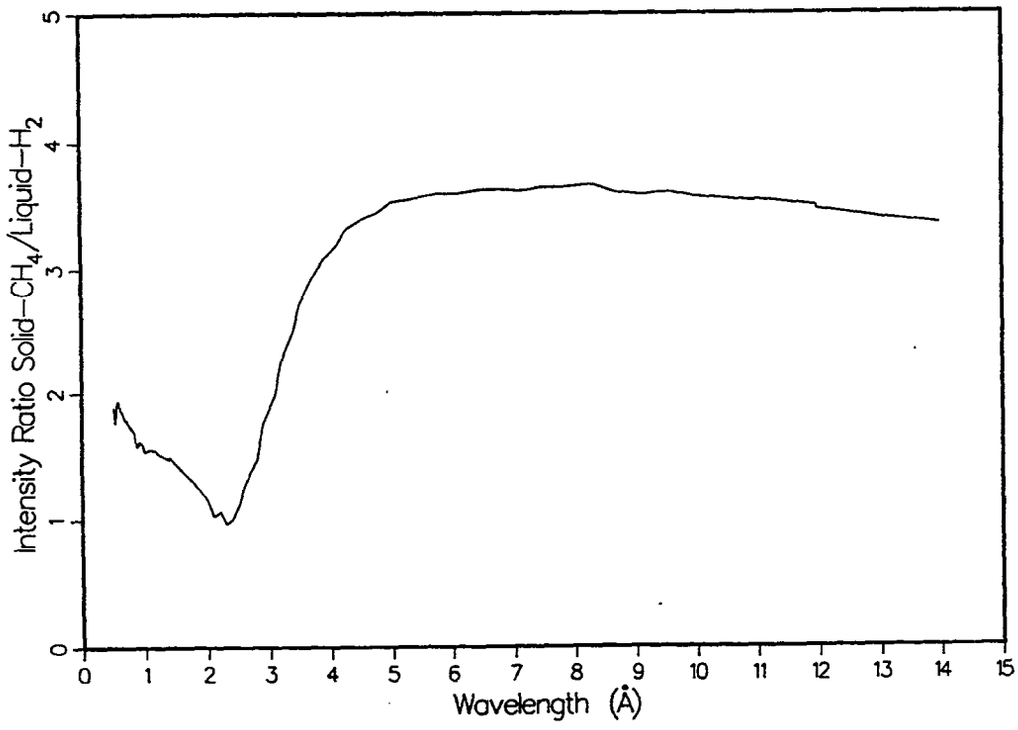

Figure 4. Ratio of the spectral intensities of solid CH_4 and liquid H_2 moderators. The same moderator can was used in both cases, and all geometry was the same.

2.3 Filter to Remove Fast Neutrons

In an instrument in which the moderator, sample, and detector are in a direct line, the very fast neutrons from the moderator can reach the detector directly. The multiple-aperture collimation used on SAND has inadequate stopping power to fully collimate such fast neutrons, so these contribute to a background halo about the main beam. Also, a very large number of such fast neutrons arrive almost simultaneously at the detector immediately after the protons strike the target, and these can produce an overload of the area detector and its

associated electronics that can affect subsequent area detector performance throughout the time frame (depending on the overload recovery time of the area detector and electronics). In SAND, a 10 cm long filter made of oriented single-crystal MgO cooled to ~80 K is located in the incident beamline. A similar MgO filter has been used on SAD for a number of years. This filter reduces the fast neutron flux by roughly two orders of magnitude, while having a transmission of ~0.5-0.7 for most of the neutrons of interest (roughly 1-14 Å). Figure 5 shows the measured transmission of the SAND MgO filter at room temperature. The cryostat for this filter is under construction, and experience with the SAD filter [4] indicates that the transmission will increase to above ~0.7 over the wavelength range of ~2-14 Å when the filter is cooled.

The MgO filter on SAND is refrigerated by a closed-loop system (CryoTiger, APD Cryogenics, Inc., Allentown, PA), and the filter and the cold head of the refrigeration system are located just inside the monolith in the outermost beamline shield block, as shown in Fig. 2. This location makes considerable use of the bulk shielding monolith for shielding against the neutrons scattered by the filter, thus minimizing the amount of external shielding which must be added. This location also allows relatively easy access to the filter and its cryostat and refrigerator for maintenance.

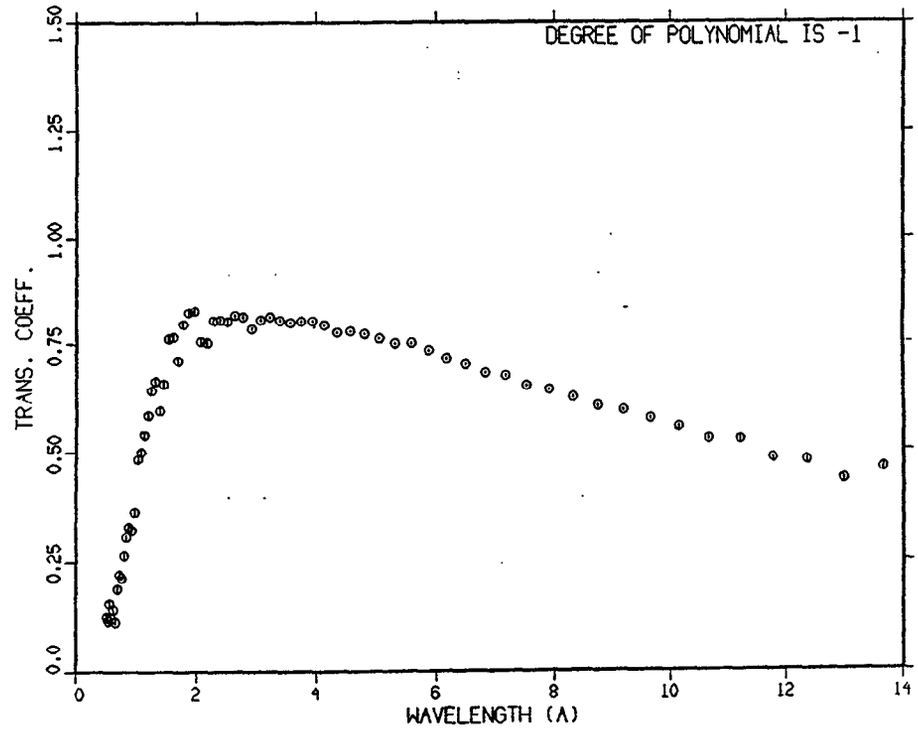

Figure 5. Transmission of the SAND single-crystal MgO filter at room temperature. Several sharp dips in the transmission in the 1-3 Å range are due to Bragg scattering in the filter.

2.4 Background Chopper

A detailed analysis [6] showed that the use of a low-speed drum chopper similar to those on the IPNS powder diffractometers SEPD and GPPD could be quite effective on the new instrument if the chopper were reduced in size and placed in the gate cavity on the C3 beamline. This chopper can be rotated at 7.5 Hz (opening twice per revolution, for a 15 Hz effective chopping frequency) in a "frame-elimination" mode to eliminate alternate prompt pulses from the 30 Hz IPNS source, providing an effectively 15 Hz operation of the instrument. In this mode the chopper also eliminates those delayed neutrons which contaminate the very-long-wavelength portion of the spectrum, so that ~16-28 Å neutrons in addition to some of the short-wavelength neutrons can be used cleanly with this chopper setting. Alternatively, the same chopper can be operated at 15 Hz (30 Hz effective chopping frequency), allowing full 30 Hz operation of the instrument, and in this mode it eliminates the delayed neutrons which normally contaminate the data from ~8-14 Å. At wavelengths below 8 Å the spectrum is sufficiently intense that delayed neutron contributions are negligible, so with this mode of operation no delayed neutron correction is required over the entire data range. The net effect is to eliminate a large background component from the long-wavelength portion of the data, thus greatly improving the signal-to-noise ratio for data over this range (delayed neutrons contribute roughly half the signal measured at TOF values corresponding to a nominal wavelength of 14 Å). Based on these simulations, an ~18.5 cm diameter drum chopper with a ~1 cm thick B_4C shell as the chopping material has been fabricated and will soon be installed in a cutout portion of the beam gate on the C3 beamline, as indicated in Fig. 2.

2.5 Collimation, Path Lengths, and Q_{min}

To achieve the necessary angular collimation in the incident beam while utilizing most of the full moderator size (~ 10 cm square) and a reasonable sample size (~ 1-2 cm diameter) requires the use of either a very long total flight path or else the use of converging multiple-aperture collimation.[2] Because of frame-overlap conditions, the maximum wavelength which can be utilized on a pulsed-source TOF instrument is

$$\lambda_{max} = \frac{3955.4}{f L_{md}} \tag{3}$$

where λ is in Å, f is the effective source frequency in Hz, and L_{md} is the total moderator-detector distance in m. A large λ_{max} helps in reaching small Q_{min}, so L_{md} must be kept as small as possible. This leads to relatively low intensities if pinhole collimation having the desired angular divergence is used, but much higher counting rates are achieved with the same angular divergence by using converging multiple-aperture collimation. If the collimation channels are all focused to the same point on the detector, then even with a short sample-to-detector distance the sample size will not affect Q_{min} or the Q-resolution.[9] Both SAD and SAND have L_{md} = 9 m, but are still able to use samples of 1 cm diameter or larger and to use neutrons from nearly all of the moderator face because of this type of collimation.

In both SAD and SAND such focusing multiple-aperture collimation is done with crossed converging Soller collimators,[2,3] as shown schematically in Fig. 6. The collimators presently available for SAND define ~ 400 converging beam channels with essentially no "dead" space between them, and provide ~0.0034 radian fwhm angular divergence (~0.007 radian full divergence) of the incident beam. The entire collimator system occupies a distance of only ~ 60 cm along the incident flight path. Figure 3 shows the physical arrangement of the collimators in their independent vacuum space, and also shows the optical system used for initial collimator and sample alignment.

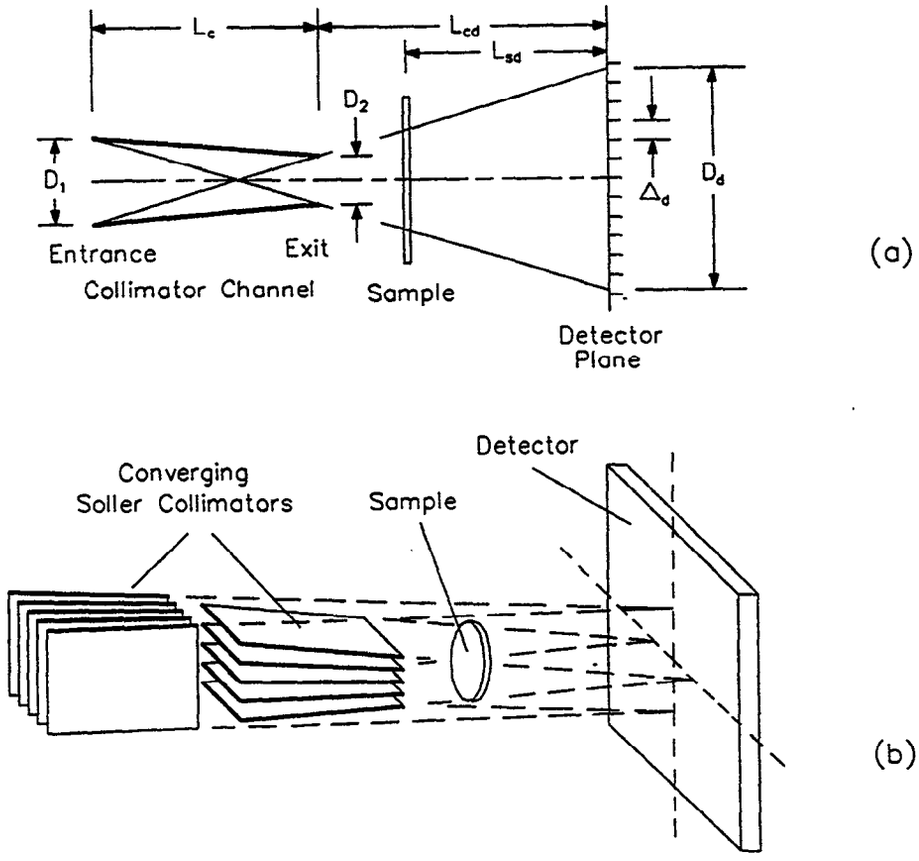

Figure 6. Schematic diagram of crossed converging soller collimators. (a) Geometry of a single collimator channel, defining some of the parameters used in the text. (b) Schematic arrangement of the crossed converging soller collimators.

The soller collimator blades are of the standard form made of stretched mylar, with ^{10}B in a suitable matrix deposited on each surface of each blade. [All collimators were purchased from Cidic, Ltd., Cheltenham, UK.] Similar collimators have been used on SAD for a number of years, and have worked quite well once the proper technique was devised for fabricating a non-reflective coating on the collimator blades.[3] It was found to be very

important to have the ^{10}B coating deposited with a rough (matte) finish in order to minimize surface reflections from the blades. Over the normal SAD operating range of 0.5-14 Å these collimators provide very low backgrounds (10^{-6} to 10^{-7} of the incident beam intensity) and produce resolutions in good agreement with the calculated values. Recent tests at IPNS with 15 Hz accelerator operation indicated that these collimators also perform well at wavelengths up to 28 Å. The multiple-aperture collimation must focus on the detector, as shown in Fig. 6, so different collimators would be needed for a different sample-to-detector distance and there is no point in having a continuously variable sample-to-detector distance in this instrument.

Upstream from the collimators, the incident beam is shaped with a series of apertures which define a circular beam with an umbra that converges from ~9 cm diameter at the moderator to a point at the detector. These apertures follow standard IPNS practice and consist of boron carbide cast with minimum epoxy. Between these apertures are thick segments of lead shot cast in epoxy containing borax and having slightly larger aperture diameters. With these apertures and the soller collimators, and with the MgO filter attenuating the fast neutrons, the resulting collimated beam has clean edges defined by the nominal geometric penumbra of the soller collimators. There is no measurable fast-neutron halo when the area detector pulse-height discrimination levels are properly set.

All channels in each soller collimator are equivalent and focus to the same spot on the area detector. Figure 6a shows the geometry associated with the focusing from a single channel of one of the soller collimators. The minimum useful scattering angle is given approximately by

$$\phi_{min} \approx \frac{\frac{B}{2} + \Delta_d}{L_{sd}} \tag{4}$$

where B is the diameter of the beamstop, Δ_d is the fwhm spatial resolution of the detector, and L_{sd} is the sample-detector distance. The beamstop must have a diameter larger than the beam penumbra diameter D_d at the detector, or

$$B = D_d + \delta \tag{5}$$

where δ is small (~2 mm or less), so this leads to

$$Q_{min} = \frac{2\pi}{\lambda_{max}} \frac{\frac{D_d + \delta}{2} + \Delta_d}{L_{sd}} \tag{6}$$

The beam penumbra size at the detector is given by

$$D_d = \frac{D_2 (L_{cd} + L_c) + D_1 L_{cd}}{L_c} \quad (7)$$

and the fwhm angular divergence of the incident beam is

$$\alpha = \frac{D_1}{L_c} \quad (8)$$

where D_1 and D_2 are the dimensions of the entrance and exit apertures of the collimator, respectively, L_{cd} is the distance from the collimator exit to the detector, and L_c is the length of the collimator, as defined in Fig. 6a.

Table 2 summarizes the values of these collimation parameters for SAD and for the current "coarse" SAND collimators. For SAND it is also intended to provide a set of "fine" soller collimators once suitable fabrication techniques can be developed. Approximate values for these collimators are included in the table as well. The measured Q_{min} for the present SAD collimators is ~0.005 $Å^{-1}$, in good agreement with the calculated value in the table, so the calculated values for SAND are expected to be fairly accurate as well. Values of Q_{min} down to ~0.003 $Å^{-1}$ and ~0.001 $Å^{-1}$ should be possible with the coarse and fine collimators for those experiments where the chopper permits useful operation with wavelengths out to 28 Å.

Table 2. Collimation Parameters for SAD and SAND[a]

		SAD[b]	SAND (coarse)[b]	SAND (fine)[c]
λ_{max}	(Å)	14	14	14
L_{sd}	(m)	1.5	2.0	2.0
L_{cd}	(m)	2.0	2.5	2.5
L_c	(m)	0.25	0.25	?[d]
D_1	(mm)	0.844	0.844	?[d]
D_2	(mm)	0.750	0.767	?[d]
D_d	(mm)	13.5	16.9	5.6[e]
α	(radian fwhm)	0.00338	0.00338	0.0011[e]
B	(mm)	15.5	19.0	8[e]
Δ_d	(mm)	~6	~6	~4[f]
Q_{min}	($Å^{-1}$) -- calculated	0.0041	0.0035	0.0022[e,f]

a. Parameters are given for the downstream (x) collimator in each case. The upstream (y) collimator parameters are somewhat different because of the different L_{cd} required, but are chosen to provide the same value of D_d as the downstream collimators.

b. Presently available.

c. Planned.

d. Final values will depend on the design and fabrication techniques selected.

e. Values in table are approximate and are based on the desired collimator performance.

f. Assumes that the nominal detector resolution can be achieved.

When both sets of collimators for SAND are available, they will be mounted on an automatic changer so that they can be easily interchanged depending on the experiment. An automated beamstop insertion mechanism has been provided on SAND to allow the use of a different beamstop size when the collimators are interchanged, in order to utilize the corresponding minimum scattering angles. This device also allows removal of the beamstop for measurements of detector sensitivity and resolution. Cadmium beamstops are used, and have adequate stopping power so long as the MgO filter is in the beam to attenuate the higher-energy neutrons.

2.6 Area Position-Sensitive Detector

SAND uses a two-dimensional rise-time-encoded position-sensitive gas-proportional-counter detector of 40×40 cm^2 active area, 2.5 cm thick and having nominally 4×4 mm^2 resolution (Ordela, Inc., Oak Ridge, TN). This detector covers the smallest scattering angles and can be operated centered on the direct beam or offset by 10 cm to increase the angular range. A gas detector was chosen because of its excellent intrinsic background characteristics, rejection of fast neutrons and gammas, and commercial availability. This detector is filled with a mixture of ^3He and CF_4 at 4 atm to provide an efficiency of ~65% at 2 Å and an intrinsic gas contribution to the position resolution of ~1.7 mm. Position and time encoding electronics for this detector duplicate those used on the present SAD. At present the measured spatial resolution is ~6 mm fwhm so there is still room for improvement in the electronics. Pulse height discrimination is used to reject any remaining fast-neutron halo around the main beam, and to eliminate the signals from gammas and electronic noise.

2.7 High-Angle LPSDs

The minimum usable wavelength with the MgO filter in the beam is ~ 1 Å. This yields usable intensity at a Q_{max} of ~ 0.5-0.6 $Å^{-1}$ when the area detector is centered on the beam. With the detector operated 10 cm off center, this is increased to Q_{max} ~ 0.8-0.9 $Å^{-1}$, at some cost in intensity at the smaller Q values. (For reference, the usable Q_{max} for SAD is ~ 0.35 $Å^{-1}$.) It is frequently desirable to have Q_{max} even larger than this, and in most cases it is desirable to sum data from a wide range of wavelengths to improve the statistics in the high-Q data. Therefore the ability to cover even higher scattering angles is incorporated into SAND by including an array of linear position-sensitive detectors (LPSDs) at higher angles. The glass-liquids-and-amorphous diffractometer (GLAD) recently built at IPNS is based entirely on such LPSDs, so the technology for position- and time-encoding a large number of such detectors is already developed.[10] This bank of LPSDs is mounted as shown in Fig 2, and will extend the range of scattering angles out to 36°. As on GLAD, a motorized absorbing bar can be driven past the upstream side of these detectors for periodic recalibration of the position encoding and resolution. Even when the wavelength range must be restricted to $\lambda > 5$ Å, as is necessary to avoid multiple-Bragg scattering for many crystalline samples, these LPSDs it should make it possible to collect good data at Q values up to ~0.7 $Å^{-1}$. Wavelengths down to 1 Å can be used for most experiments, and in this case good counting statistics should be possible at Q values up to 1 $Å^{-1}$ or more.

2.8 Beam Monitors and Measurement of Sample Transmissions

The incident beam monitor is a low-efficiency BF_3 ionization chamber, similar to that used on most of the other IPNS instruments. It is located just upstream from the soller collimators (see Fig. 3).

Sample transmissions are measured by means of a gas proportional counter detector having an efficiency of ~0.1 for 2 Å neutrons. For transmission measurements this detector is automatically lowered into the transmitted beam just in front of the beamstop (see Fig. 2), while for scattering measurements it is automatically raised outside the path of the scattered neutrons.

Development is underway on a small detector which can be placed just upstream from the beamstop. This monitor detector is smaller than the diameter of the beamstop, so that it is totally masked from the area detector by the beamstop. If this detector proves successful it will replace the insertable transmission monitor, making it possible to measure transmissions concurrently with the scattering measurements.

2.9 Alignment and Calibration

An optical alignment system has been built into SAND in order to facilitate alignment of the soller collimators, beamstop, and transmission monitor. This system, shown in Fig. 3, includes a halogen lamp as a broad white-light source and a low-power laser for finer alignment. Both are directed along the surveyed axis of the instrument by a thin (3 mm thick) single-crystal silicon wafer permanently mounted in the neutron beam upstream from the soller collimators, and inclined at 45° to the beam. This wafer has minimal effect on the neutron beam. . The laser beam is first reflected by a thin glass plate in front of the halogen lamp (see Fig. 3), and then directed along the instrument axis by the silicon mirror. The vacuum windows at the entrance and exit of the soller collimator chamber, and at the entrance to the scattering chamber are all made of high-quality single-crystal sapphire (HEMEX quality, from Crystal Systems, Inc., Salem, MA). These windows have good neutron transmission and are optically transparent, so the light from the halogen lamp or from the laser can be transmitted all the way to the area detector.

The broad white-light source illuminates all the slits of the soller collimators, and so provides a good representation of the entire collimated beam. Either this light source or the laser can be used to align the soller collimators so that the transmitted beam is centered on the sample position and on the optical axis at the detector. The laser is then used to provide the initial centering of the beamstop and the transmission monitor, before their alignment is fine-tuned using the neutron beam. This optical system has reduced the alignment process to a matter of a few minutes.

The white-light source provides good images of any apertures placed near the sample, so the exact portion of the sample being illuminated by the light, and hence by the neutron beam,

can be determined. For non-standard sample equipment, the laser and white-light sources provide a means for quick centering of the sample in the beam.

The encoding of the area detector and LPSDs is periodically checked for linearity and resolution by measurement of uniform flood patterns with and without masks in front of the detectors. This is usually done with a moderated Pu-Be source at the sample position. The beamstop and transmission monitor can be withdrawn so that the entire area detector can be illuminated by this source. A hinged mask can be swung into place in front of the area detector, and a motorized absorbing bar can be driven in front of the LPSDs, and patterns measured with these masks in place enable the position encoding and the resolution of the detectors to be indexed on an absolute scale.[8,10] All of these measurements can be made during scheduled accelerator down time, so that no beam time is wasted.

2.10 Effects of Gravity

Because of gravity a neutron beam of wavelength λ traveling a distance L falls a distance

$$y = \frac{gt^2}{2} = \frac{g}{2}\left(\frac{m}{h}\right)^2 L^2 \lambda^2 = 3.132 \times 10^{-4} L^2 \lambda^2 \qquad (13)$$

where g = 980 cm·sec^{-2}, and y is in cm, L in m, and λ in Å. For L = 2.5 m, the distance from the collimator exit to the area detector on SAND, the maximum fall is y = 0.38 mm at λ = 14 Å. Thus for 30 Hz operation all gravitational effects are small enough to be ignored. If the chopper is operated in frame-elimination mode to allow use of neutrons out to 28 Å, then the maximum gravitational fall will reach 1.5 mm for the longest wavelengths, necessitating the use of slightly elongated beamstops and minor wavelength-dependent corrections to the scattering angle to account for this drop.

2.11 Sample Environment

A large sample region is provided in the instrument, with proper alignment fixtures so that a wide variety of sample environments can be easily interchanged in the instrument. Included among these are cryogenic capabilities, temperature-controlled sample changers, furnace capabilities with the sample in vacuum or a controlled atmosphere, high pressure cells, and magnetic fields.

Figure 3 shows details of the sample chamber. The incident flight path has its own independent vacuum, which is terminated downstream from the last soller collimator by a single-crystal sapphire vacuum window. A second sapphire window at the entrance to the scattering flight path isolates the scattering flight path vacuum from the sample area, while introducing little additional background in the scattering pattern. The use of sapphire windows permits optical alignment of the various instrument components. For most samples, the path between these windows will be in air. Both of the sapphire windows can be removed and the sample area can be evacuated when it is desired to minimize the window and air scattering, or when bulky sample-environment equipment is in use. The top flange

on the sample chamber conforms to IPNS standards, and ensures precise centering of the sample in the beam when top-mounting sample equipment (e.g., closed-cycle refrigerator) is used.

2.12 Data Acquisition System

The data acquisition system is essentially a duplicate of other IPNS data acquisition systems,[10,11] with some modifications to allow operation of both the area detector and the LPSDs on the same system.

2.13 Data Analysis

Because it is necessary to use the TOF technique at pulsed sources, data are collected as functions of the x and y coordinates on the detector and of the time-of-flight t, which is proportional to the neutron wavelength. The resulting x-y-t data sets can contain on the order of a million elements, or even considerably more when LPSDs are used to supplement the angular range, so considerable attention must be given to data collection and analysis. Analysis programs for reducing the TOF SANS data from SAD have been in routine use for a number of years, and are currently used to analyze data from the SAND area detector. Development of the software to smoothly combine the area detector and LPSD data is now underway.

3. Performance

SAND is just now being commissioned, so its measured performance can not yet be discussed in detail. However, at least in the initial stages it is expected to have performance similar to or better than SAD. Therefore we discuss briefly the operation of SAD and the quality of data obtained, and then indicate areas in which SAND will likely provide improvements.

3.1 Data Reduction

In a typical scattering experiment at the SAD, prompt neutrons with wavelengths between 0.5 and 14 Å are used. The scattering data are binned in 67 time slices, with $\Delta\lambda/\lambda = 0.05$, and for each time slice the data are stored in a 64×64 spatial array. These binning parameters, however, may be altered at the discretion of the user, depending on the resolution requirement. In order to express the SANS data in terms of the sample's absolute differential cross section, one needs the scattering data from the sample and its background, the wavelength-dependent transmission coefficients for the sample and its background, thickness of the sample, the detector sensitivity and nonlinearity of the pixels of the area detector, spectral distribution of the probing neutrons and a scale factor to account for certain unscaled parameters.

Because one wishes to combine the information from the different wavelength bands (time slices) into the more conventional S(Q) array, it is necessary to determine the wavelength distribution of neutrons in the beam for use in normalization. This measurement is carried

out using the area detector, with the beam stop removed and with the incident beam intensity attenuated by a cadmium mask filled with tiny holes. This mask protects the detector by attenuating the beam intensity, without altering the spectral character of the neutron beam.

The wavelength-dependent sample transmission coefficient is defined as the ratio of the sample attenuated neutron beam to that of the unattenuated beam. It is determined in a separate measurement by inserting a high-efficiency transmission monitor detector in front of the beam stop.

The data on the wavelength dependent transmission coefficients for the sample and the background, efficiency-weighted source spectrum, relative detector sensitivity, and the measured raw scattering data for the sample, background, and cadmium blank are sufficient to determine the net normalized scattering data in each encoded detector element. The full measured time spectrum for each pixel provides the necessary information to correct the data for the effects of delayed neutrons,[5] if this is important. Dividing the net scattering values by the thickness of the sample and multiplying by a scale factor converts the measured scattering of the unknown sample to absolute cross sections. The scale factor is determined from measurements of a standard sample whose absolute scattering cross-section is available. At IPNS we use a polymer melt sample (Bates poly) which consists of a 50:50 volume mixture of hydrogenous and deuterated high molecular weight polystyrene for this purpose. The data can then be remapped as S(Q) by using the known values of the bin widths of the encoded cells and the wavelengths corresponding to each of the time slices. These resulting S(Q) values are on an absolute scale in the units of cm^{-1} per steradian.

3.2 Example of SAD Data

As an example, Figure 7 shows data measured for a 5.5 mM GroEL in D_2O measured at the 30m SANS instrument at ORNL and at SAD at IPNS.[12] GroEL is a chaperonin which identifies and binds with proteins denatured under stress. The SAD data have been reduced and placed on an absolute scale using the procedure described above. While the SANS data from the ORNL instrument has been measured at 12 m and 3 m sample-to-detector settings for a total of 5.5 hr in a 0.5 cm thick Suprasil cell, the SAD data was measured in a single setting for 4 hr in 0.2 cm thick Suprasil cell. There is excellent agreement, on an absolute scale, between the low-Q ORNL data and that from SAD, although the density of points in the low Q region in the ORNL data is about 3 times larger than that in the SAD data.

However, this example illustrates the importance of measuring over the full Q range in a single experiment whenever time-dependent variations can occur in the sample. This protein complex in solution can change with time due to a change in the subunit-complex equilibrium,[12] depending on the handling and storage conditions. Since SAD data for other, stable, samples agree with ORNL data over the entire Q range, the small discrepancies at higher Q in these particular data sets suggest a possible time-dependent change in the sample between the measurements with the two different settings on the ORNL instrument. Thus the SAD data were necessary in order to be able to properly assess the relative magnitudes of the low-Q and high-Q portions of the scattering.

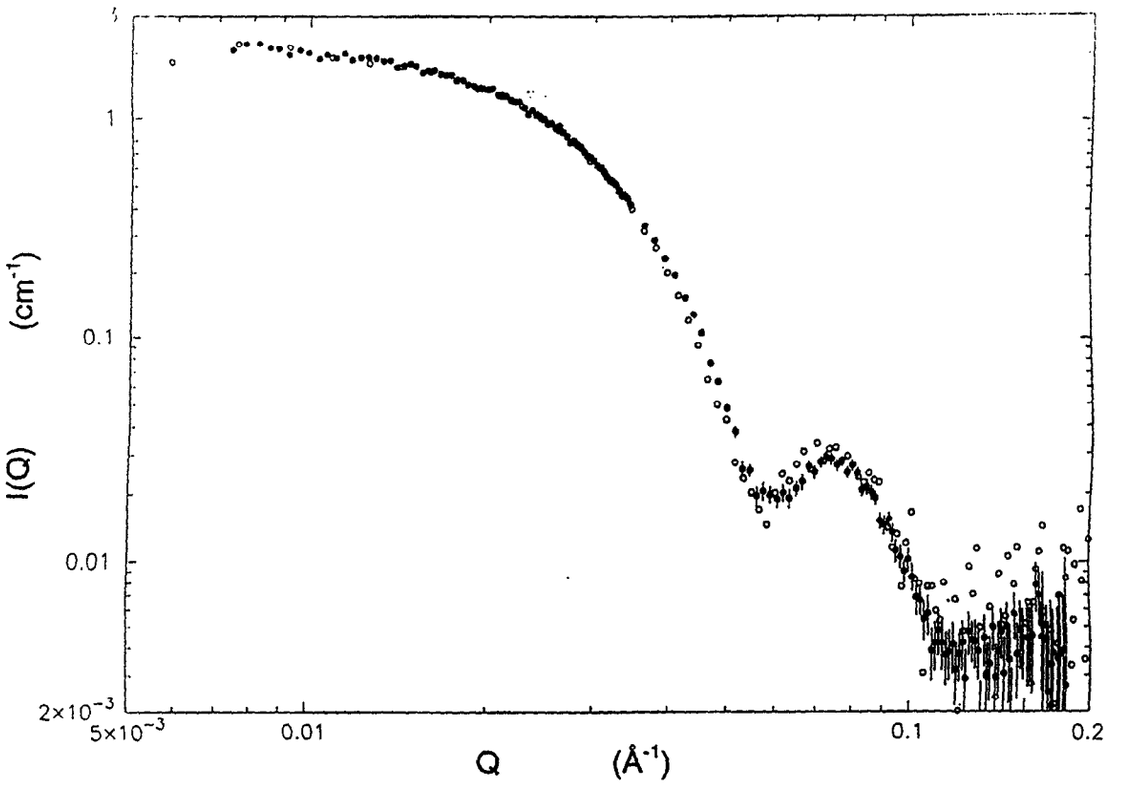

Figure 7. SANS data for E. coli GroEL from SAD (open circles) and from the 12-m and 3-m settings of the 30 m SANS instrument at ORNL (closed circles).

3.3 Expected Improvements with SAND

As is suggested in Fig. 7, much of the interesting data lies at the higher Q values, above 0.1 $Å^{-1}$. The present SAD already provides data in this region comparable to that from ORNL. Even so, the statistics are too poor to do much with the data above 0.1 $Å^{-1}$ in this example. More and more of the experiments being proposed are of this type, and would greatly benefit from an extension of the Q range to higher Q values. The larger area detector on SAND will lead to factors of 2-4 increase in measured intensity in this Q range, and the inclusion of the LPSDs on SAND will provide as much as an order of magnitude additional intensity at these and even higher Q values. This should open up an exciting new range to further exploration.

At present, SAD cannot reach Q values below 0.005 $Å^{-1}$, as can be seen in Fig. 7. This low-Q range is also important for many experiments. When SAND is fully operational, the capability to use wavelengths out to 28 Å and the availability of a set of fine soller collimators should extend the range down to 0.002 $Å^{-1}$ or possibly even to 0.001 $Å^{-1}$.

4. Summary

A new small-angle neutron diffractometer SAND at IPNS is now being commissioned. This instrument builds upon the more than 15 years experience with pulsed neutron small-angle diffraction at IPNS, and incorporates many new features to improve both Q_{min} and Q_{max} as well as improving the ease of instrument operation. The area-detector portion of SAND is expected to be operational with the coarse soller collimators in late 1995. The chopper is being bench-tested, and will also be incorporated in the instrument in 1995. It is expected that SAND will be placed in the user program in this configuration in Spring, 1996. The schedule calls for bringing the LPSD bank on line in late 1996. The last item to be added will be the set of fine soller collimators, and the schedule for these will depend on the outcome of the efforts to develop the appropriate fabrication technology.

Acknowledgments

The authors would like to thank the National Science Foundation and Professor S.-H. Chen of the Massachusetts Institute of Technology for a grant which aided in the development of some of the instrument concepts for SAND, and would also like to thank the Texaco Corporation for a grant that funded part of the construction of SAND.

References

[1] J. M. Carpenter, U. Walter, and D. F. R. Mildner. Proceedings of the 9th Meeting of the International Collaboration on Advanced Neutron Sources (ICANS IX), Swiss Institute for Nuclear Research, Villigen, Switzerland, Sept. 22-26, 1986. Swiss Institute for Nuclear Research report ISBN 3-907998-01-4, 1987, pp. 279-303.

[2] R. K. Crawford and J. M. Carpenter. *J. Appl. Cryst.* **21** (1988) 589-601.

[3] R. K. Crawford, J. E. Epperson, and P. Thiyagarajan. *Advanced Neutron Sources 1988*, Proceedings of the 10th Meeting of the International Collaboration on Advanced Neutron Sources (ICANS X), Los Alamos National Laboratory, Oct. 3-7, 1988. Institute of Physics Conference Series Number 97, IOP Publishing Ltd, New York, 1989, pp. 419-426.

[4] J. M. Carpenter, D. F. R. Mildner, S. S. Cudrnak, and R. O. Hilleke. *Nucl. Instrum. Methods* **A278** (1989) 397-401.

[5] J. E. Epperson, J. M. Carpenter, P. Thiyagarajan, and B. Heuser. *Nucl. Instrum. Methods* **A289** (1990) 30-34.

[6] R. K. Crawford, J. E. Epperson, P. Thiyagarajan, and J. M. Carpenter. Proceedings of the 11th Meeting of the International Collaboration on Advanced Neutron Sources (ICANS XI National Laboratory for High Energy Physics, Tsukuba, Japan, Oct. 22-26, 1990. KEK report 90-25, 1991, pp. 873-889.

[7] J. M. Carpenter, D. F. R. Mildner, J. W. Richardson, Jr., and W. C. Dimm. Proceedings of the 11th Meeting of the International Collaboration on Advanced Neutron Sources

(ICANS XI), National Laboratory for High Energy Physics, Tsukuba, Japan, Oct. 22-26, 1990. KEK report 90-25, 1991, pp. 1044-1053.

[8] R. K. Crawford, P. Thiyagarajan, and J. Chen. Proceedings of the 12th Meeting of the International Collaboration on Advanced Neutron Sources (ICANS XII), Abingdon, UK, May 24-28, 1993. Rutherford Appleton Laboratory report 94-025, 1994, pp. I208-I215.

[9] A. C. Nunes. *Nucl. Instrum. Methods* **119** (1974) 291-293.

[10] R. K. Crawford and J. R. Haumann. *IEEE Trans. Nucl. Sci.* **NS-37** (1990) 72-81.

[11] J. R. Haumann and R. K. Crawford. *IEEE Trans. Nucl. Sci.* **NS-34** (1987) 948-953.

[12] P. Thiyagarajan, S. J. Henderson, and A. Joachimiak. *Structure*, (1995) in press.